*Macromolecular Chemistry and Physics*

Macromolecular Chemistry and Physics
www.mcp-journal.de

RESEARCH ARTICLE OPEN ACCESS

# A Gel Polymer Electrolyte Housed in a Tetronic-Based Model Amphiphilic Polymer Conetwork Matrix

Demetris E. Apostolides[1] | Costas S. Patrickios[1] | Yinghui Zhang[2] | Shanshan Yan[2] | Benoît Notredame[2] | Jean-François Gohy[2]

[1]Department of Chemistry, University of Cyprus, Nicosia, Cyprus | [2]Institute of Condensed Matter and Nanoscience (IMCN), Bio- and Soft Matter (BSMA), Université catholique de Louvain (UCL), Louvain-la-Neuve, Belgium

**Correspondence:** Costas S. Patrickios (costasp@ucy.ac.cy)

**Received:** 6 September 2025 | **Revised:** 19 December 2025 | **Accepted:** 5 January 2026

**Keywords:** acylhydrazone | amphiphilic polymer conetworks | electrochemical stability | gel polymer electrolytes | ion conductivity | ionogels | lithium-ion batteries

## ABSTRACT

An appropriately end-functionalized amphiphilic four-armed star diblock copolymer comprising hydrophilic poly(ethylene glycol) (PEG) external blocks (80 mol%) and hydrophobic poly(propylene glycol) (PPG) inner blocks (20 mol%), Tetronic T1107, of a molar mass of 15 000 g mol$^{-1}$ was used to form a model amphiphilic polymer conetwork (APCN) containing an ionic liquid mixture with lithium and imidazolate cations. The resulting ionogel was characterized in terms of its ionic conductivity, relevant to its potential employment as a gel polymer electrolyte in lithium-ion batteries. To this end, a series of samples were formulated, differing in the initial overall concentration of star diblock copolymers in the reaction mixture, the stoichiometry between the two reactive star polymer end-groups, and the catalyst concentration. An optimal room temperature ionic conductivity of 0.4 mS cm$^{-1}$ was exhibited by a particular formulation, attributed to a combination of a lower network crosslinking density and a higher (final) volume fraction of the ionic liquid mixture. This maximum room temperature ionic conductivity value compares favorably with the corresponding values measured for similar ionogels housed in APCNs based on Pluronics and four-armed PEG stars.

## 1 | Introduction

Ionogel electrolytes are generally recognized as promising electrolytes for application in electrochemical devices, in which ionic liquids are immobilized by a solid matrix [1]. Ionic liquids are molten salts composed of cationic and anionic species with a melting point below 100°C [2–4]. Ionogel electrolytes inherit the favorable properties of ionic liquid including outstanding ionic conductivity, negligible vapor pressure, nonflammability and nonvolatility, favorable electrochemical and thermal properties [5]. The solid matrices for ionogel electrolytes are required to be chemically inert to avoid harmful reactions with ionic liquids. A wide range of solid matrices have been explored, consisting of polymeric, inorganic and hybrid materials [6]. Ionogel electrolytes based on polymer matrices are mostly studied, in which polymer matrices include poly(ethylene glycol) (PEG), poly(vinylidene fluoride) (PVDF) and poly(methyl methacrylate) (PMMA), as well as poly(vinylidene difluoride-*co*-hexafluoropropylene) (PVDF-HFP) [6, 7]. Ionogel electrolytes cannot only overcome the fluidity of ionic liquids but also exhibit the high mechanical strength of solid matrices, which enhances the safety and elevates the high-temperature limit of battery operation [8].

Ionic conductivity is a key metric of ionogel electrolytes, which has a decisive effect on the rate capability of lithium-ion batteries. Solid polymer electrolytes are required to withstand elevated temperatures to attain adequate ionic conductivity for rechargeable lithium-ion batteries. However, ionogel electrolytes have shown favorable ionic conductivity at room temperature as quasi-solid-

state electrolytes, which has led to desirable rate performance at room temperature for lithium-ion batteries [1]. Lithium-ion transfer number ($t_{Li}^+$) is an important parameter for evaluating ionogel electrolytes, because it is vital to prevent anion over migration. However, ionogel electrolytes are characterized by a low $t_{Li}^+$, which leads to adverse side reactions and impedes the cycling life of lithium-ion batteries [9]. The $t_{Li}^+$ of ionogel electrolytes can be improved by increasing the lithium-ion transport paths and strengthening the interactions between solid matrices and ionic liquids [6]. The electrochemical stability of the ionogel electrolyte is important to maximize voltage and energy density of the lithium-ion battery. Traditional liquid electrolytes are insufficiently stable for high voltage cathode materials, but ionogel electrolytes have shown a wide electrochemical stability window close to 5.0 V (vs. $Li/Li^+$) that originated from the high electrochemical stability of ionic liquids, which can match with high-voltage cathode materials, achieving high-output voltage for lithium-ion batteries [2, 6]. In comparison with ionic liquid electrolytes, ionogel electrolytes show superior mechanical properties and favorable interfacial stability with lithium metal.

The application of ionogel electrolytes in lithium-ion batteries has been studied for about two decades. As a typical example, Chen et al. synthesized an ionogel electrolyte with interpenetrating polymer double-network (DN) structure by UV-crosslinking, in which the second poly(methoxyPEG acrylate) network was successfully introduced into the initial polymer network of PVDF-HFP [10]. The optimal ionogel electrolyte exhibited an outstanding room temperature ionic conductivity of $1.2 \times 10^{-3}$ S cm$^{-1}$, high decomposition voltage and excellent mechanical strength, as well as a good interface compatibility with lithium metal. The corresponding $LiFePO_4$|ionogel|Li cell showed an outstanding initial specific discharge capacity and excellent cycle stability. In another study, Liang et al. developed a DN ionogel electrolyte (DN-Ionogel) by a facile one-step crosslinking method, in which 1-ethyl-3-methylimidazolium bis(trifluoromethyl)imide (EMIM-TFSI) was trapped into the DN made of a poly(ionic liquid) and PVDF-HFP [11]. Benefiting from the DN architecture, the ionogel electrolyte exhibited a remarkable ionic conductivity of $1.8 \times 10^{-3}$ S cm$^{-1}$ and wide electrochemical window (up to 5.0 V) at room temperature as well as favorable mechanical properties. The $LiFePO_4$|DN-Ionogel|Li cell delivered high charge/discharge capacity and superior rate performance as well as stable cyclic performance. As another example, Zhao et al. synthesized a novel chemically crosslinked ionogel electrolyte based on an acrylated hyperbranched polymer and ionic liquid of BMIM-$BF_4$ by photopolymerization [12]. The ionogel electrolyte exhibited enhanced mechanical properties and high thermal stability as well as satisfactory electrochemical performance. The $LiFePO_4$|Li batteries fabricated with this ionogel electrolyte showed stable charge/discharge behavior and good cycle stability.

Thus, the ionogel polymer matrices are crosslinked, thereby possessing a polymer network architecture [13]. Most of those polymer network matrices are randomly crosslinked, having a poorly-defined structure. From the small number of studies in which the polymer network matrix is well-defined, most of these are on homopolymer materials, such as model networks [14, 15] based on end-linked four-armed PEG (tetraPEG) stars, i.e., tetraPEG gels [16–19]. With only one polymeric component, this must be the polar one, compatible with the ionic liquid, and should facilitate ion pair separation. Not having a second polymeric component, this deprives the ionogel system from acquiring a second function, such as mechanical property enhancement, already done in the DN systems mentioned above [10, 11] which, however, do not possess a model network structure. To our knowledge, there are only two studies [20, 21] in the literature, describing ionogels with well-defined polymer matrices composed of two components. These two-component polymer network matrices, whether well-defined or not, are called amphiphilic polymer conetworks (APCNs) [22–52], because these two components are usually mutually incompatible. In the first of the two above-mentioned studies, the ionogel is housed within a well-defined APCN matrix obtained by the end-linking of two different types of four-armed star homopolymers: PVDF (tetraPVDF star) and PEG (tetraPEG star), with the former providing mechanical robustness due to its semi-crystallinity (it is also moderately polar), and the latter being capable to dissolve within the ionic liquid due to its polarity [20]. In the second example, the well-defined APCN matrix comprised an end-linked linear amphiphilic Pluronic ABA triblock copolymer, with a central poly(propylene glycol) (PPG), rather hydrophobic (and less polar) block, flanked by two polar PEG blocks [21].

In the present ionogel study, we keep a well-defined APCN matrix to house the ionic liquid but expanded on the design of the matrix by exploring a different building block architecture. Thus, instead of employing two different star homopolymer types or a linear amphiphilic block copolymer, we adopt an amphiphilic star block copolymer architecture. In particular, we make use of a four-armed star diblock copolymer with inner poly(propylene glycol) PPG blocks (20%), and peripheral PEG blocks (80%), an overall molar mass of 15 kDa, and hydroxyl terminal groups. This is a commercially available star polymer sample called Tetronic T1107 [53]. Being a star polymer, this material would not only serve as the main building block, but also as the crosslinker. Although other types of Tetronic samples have been used to prepare well-defined APCNs [54–57], none of those APCNs has been used to host an ionic liquid, a task undertaken in this investigation.

This work first involved the end-functionalization of the Tetronic four-armed star block copolymer, so as to produce two derivatives, differing only in their terminal groups. These two types of terminal groups were chosen to be reactive to each other, enabling network formation upon the mixing of the two Tetronic derivatives. The second step was indeed the mixing of solutions of these mutually reactive Tetronic derivatives, but also in the presence of the ionic liquid, which, due to its low volatility, remains entrapped within the APCN ionogel even upon solvent vacuum evaporation. Third, various APCN ionogel formulations, cast as films, were characterized in terms of their ionic conductivity, and the formulation with the highest conductivity was identified, attributing this optimal behavior to certain formulation properties. Finally, the best ion conductivity value measured for this APCN ionogel system is compared to those of similar APCN ionogel systems.

## 2 | Experimental Section

### 2.1 | Materials

T1107 Tetronic [ethylenediamine tetrakis(propoxylate-*block*-ethoxylate) tetrol], methanesulfonyl chloride

**TABLE 1** | Exact quantities of the various components used for the different formulations.

| Sample | | T-Bz : T-Ac | % w/v polymer | ac. ac.[b] (% v/v) | T-Bz[a] (μL) | T-Ac[a] (μL) | ac. ac.[b] (μL) | DMF (μL) | IL (μL) |
|---|---|---|---|---|---|---|---|---|---|
| No. | Name | | | | | | | | |
| 1 | 1:1_5_5 | 1:1 | 5 | 5 | 125 | 125 | 50 | 630 | 70 |
| 2 | 1:1_10_5 | 1:1 | 10 | 5 | 250 | 250 | 50 | 380 | 70 |
| 3 | 1:1_5_5′ | 1:1 | 5 | 5 | 62.5 | 62.5 | 25 | 315 | 35 |
| 4 | 1:1_5_5′ | 1:1 | 10 | 5 | 125 | 125 | 25 | 190 | 35 |
| 5 | 2:3_10_5 | 1:1.5 | 10 | 5 | 100 | 150 | 25 | 190 | 35 |
| 6 | 3:2_10_5 | 1.5:1 | 10 | 5 | 150 | 100 | 25 | 190 | 35 |
| 7 | 1:2_10_5 | 1:2 | 10 | 5 | 83.5 | 166.5 | 25 | 190 | 35 |
| 8 | 2:1_10_5 | 1:1 | 10 | 5 | 166.5 | 83.5 | 25 | 190 | 35 |
| 9 | 1:1_15_5 | 1:1 | 15 | 5 | 185 | 185 | 25 | 70 | 35 |
| 10 | 1:1_15_10 | 1:1 | 15 | 10 | 185 | 185 | 50 | 45 | 35 |
| 11 | 1:2_11_5 | 1:2 | 11 | 5 | 92.5 | 185 | 25 | 162.5 | 35 |
| 12 | 2:1_11_5 | 2:1 | 11 | 5 | 185 | 92.5 | 25 | 162.5 | 35 |

[a]20% w/v DMF solutions.

[b]ac. ac.: acetic acid.

(≥99.7%), 4-hydroxybenzaldehyde (98%), *N*′-benzylidene-4-hydroxybenzohydrazide (99%), hydrazine hydrate (80%), triethylamine (TEA, ≥99.5%), anhydrous magnesium sulfate (≥99.5%), sodium hydrogen carbonate ($NaHCO_3$, ≥99.7%), aqueous sodium hydroxide (1 M), calcium hydride ($CaH_2$, 90%–95%), glacial acetic acid (≥99.7%), *N*,*N*-dimethylformamide (DMF, 99.8%), dichloromethane (≥99.8%, DCM), dimethylsulfoxide (≥99.9%), 1,4-dioxane (≥99%), diethyl ether (≥99.5%), and dialysis tubing composed of benzoylated cellulose with molar mass cut-off of 3000 g $mol^{-1}$ (average flat width 32 mm) were purchased from Sigma–Aldrich–Merck, Germany. The ionic liquid mixture, comprising two organic salts, lithium bis(trifluoromethanesulfonyl)-imide (LiTFSI) and 1-ethyl-3-methylimidazolium bis(trifluoromethanesulfonyl)-imide (EMIM-TFSI), combined at a 1: 9 LiTFSI: EMIM-TFSI molar ratio, was purchased from Solvionic in Toulouse, France.

## 2.2 | T1107 Tetronic End-Functionalizations

The starting T1107 Tetronic (T-OH) was derivatized to its two mutually reactive forms, T-Bz and T-Ac, following our previously published procedures developed for the derivatization of Tetronic T904 [57], tetraPEG star [20, 58] and Pluronic F108 [21], albeit with small changes depending on solubilities in the various solvents. Confirmation of the structure of the two final products, T-Bz and T-Ac, was obtained using $^1$H NMR spectroscopy, whereas details of the synthesis will be provided in a following publication.

### 2.2.1 | $^1$H NMR Spectrum of T-Bz in $CDCl_3$ ($\delta$)

1.15 ppm (broad, $CH_2CH(CH_3)O$, 240 H), 3.4 ppm (broad, $CH_2CH(CH_3)O$, 80 H), 3.6 ppm (broad, $CH_2CH(CH_3)O$, 160 H), 3.7 ppm (broad, $CH_2CH_2O$, 944 H), 3.9 ppm (t, $CH_2CH_2O$-terminal group, 8 H), 4.25 ppm (t, $CH_2CH_2O$-terminal group, 8 H), 7.0 ppm (d, aromatic, 8 H), 7.9 ppm (d, aromatic, 8 H), 9.9 ppm (s, O—C*H*, 4 H).

### 2.2.2 | $^1$H NMR Spectrum of T-Ac in DMSO-$d_6$ ($\delta$)

1.0 ppm (broad, $CH_2CH(CH_3)O$, 240 H), 3.3 ppm (broad, $CH_2CH(CH_3)O$, 80 H), 3.4 ppm (broad, $CH_2CH(CH_3)O$, 160 H), 3.5 ppm (broad, $CH_2CH_2O$, 944 H), 3.7 ppm (t, $CH_2CH_2O$-terminal group, 8 H), 4.1 ppm (t, $CH_2CH_2O$-terminal group, 8 H), 4.3 ppm (s, $NHNH_2$, 8 H), 7.0 ppm (d, aromatic, 8 H), 7.8 ppm (d, aromatic, 8 H), 9.6 ppm (s, $NHNH_2$, 4 H).

## 2.3 | Ionogel Preparation

Separate 20% w/v solutions of the T-Bz and T-Ac star polymer building blocks were prepared in DMF. The appropriate volume of the ionic liquid mixture (IL) was added, dissolved in extra DMF, to the T-Bz DMF solution, whereas the appropriate volume of the glacial acetic acid catalyst was added to the T-Ac DMF solution. The specific amounts (volume) of each component are given in Table 1 below.

## 2.4 | Ion Conductivity Measurements

The conductivity measurements were conducted using the following parameters: frequency range from 50 mHz to 1 MHz, Nd: 8 points per decade, and Va = 10.0 mV. The temperature program followed the sequence 20°C – 60°C – 50°C – 40°C – 30°C – 20°C – 80°C – 20°C, with a 2 h of resting at each temperature to ensure homogeneity in the sample's temperature. Each ionogel membrane had a thickness of approximately 200 μm.

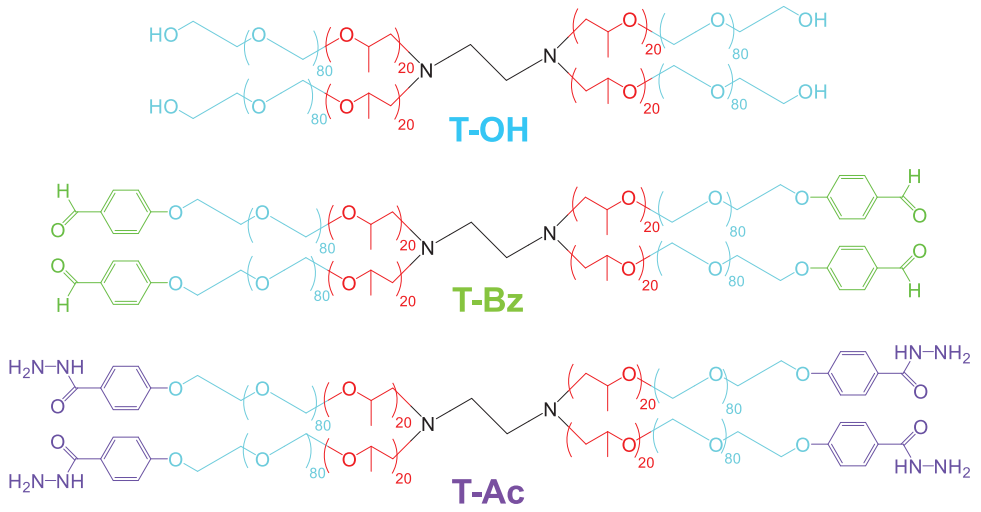


**FIGURE 1** | Chemical structures of the starting T1107 Tetronic four-armed star diblock copolymer, T-OH, and the two types of its end-functionalized derivatives, T-Bz and T-Ac, which are mutually reactive.

## 3 | Results and Discussion

### 3.1 | End-functionalized Polymer Building Blocks

Figure 1 illustrates the chemical structures of the starting T1107 Tetronic four-armed star block copolymer with four hydroxyl terminal groups, T-OH, and its two derivatives, T-Bz and T-Ac, which constitute the main building blocks for the presently prepared and characterized APCN-based ionogel. These two derivatives differ only with respect to their four end-groups which were chosen to be reactive to each other in order to enable network formation. The one type of end-group is benzaldehyde (Bz), whereas the other is benzaacylhydrazide (Ac) which, under acidic conditions, may quantitatively react with the benzaldehyde end-group to yield a bis-aryl substituted acylhydrazone group [59–61]. This is not only a type of a "click" reaction, but it is also an exchange reaction whose exchange rate may be regulated through pH. The details for the end-functionalization can be found in our previously published work [57]. Briefly, the hydroxyl end-groups of the starting T1107 Tetronic were first activated by mesylation. In the case of the Bz-derivatized sample (T-Bz), the installed mesyl groups were displaced using excess of 4-hydroxybenzaldehyde. In the case of the Ac-derivatized sample (T-Ac), the mesyl groups were displaced using excess of benzaldehyde-protected 4-hydroxybenzhydrazide. After its purification, the latter (intermediate) product was subjected to hydrazinolysis, using a large excess of hydrazine, at room temperature, to yield T-Ac which was first purified by dialysis against water and then lyophilized.

### 3.2 | Combination of Polymer Building Blocks for APCN Ionogel Formation

Figure 2 schematically depicts the APCN formation through the combination of its two polymeric building blocks, T-Bz and T-Ac, whose prior preparation, via appropriate end-functionalization of the starting T-OH, is also sketched in the figure.

Because the two end-functionalized derivatives of T-OH, T-Bz and T-Ac, are water-soluble, APCN formation may be performed in water and obtain APCN hydrogels. However, for the purposes of the present study, ionogel formation must be performed in the absence of water. Thus, APCN ionogel formation was performed in a polar organic solvent, in the presence of the ionic liquid (an ionic liquid mixture, to be precise) and a small amount of acid to catalyze the acylhydrazone bond formation reaction, to lead to crosslinking and obtain the network. *N*,*N*-dimethylformamide (DMF) was the polar organic solvent used, whereas glacial acetic acid was the chosen acid catalyst. The ionic liquid mixture comprised two liquid organic salts, lithium bis(trifluoromethanesulfonyl)imide (LiTFSI) and 1-ethyl-3-methylimidazolium bis(trifluoromethanesulfonyl)imide (EMIM-TFSI), combined at a 1:9 molar ratio. For ionogel formation, separate 20% w/v solutions of T-Bz and T-Ac in DMF were prepared and mixed. The T-Bz DMF solution also contained the ionic liquid mixture, whereas the T-Ac DMF solution also contained the acetic acid crosslinking catalyst.

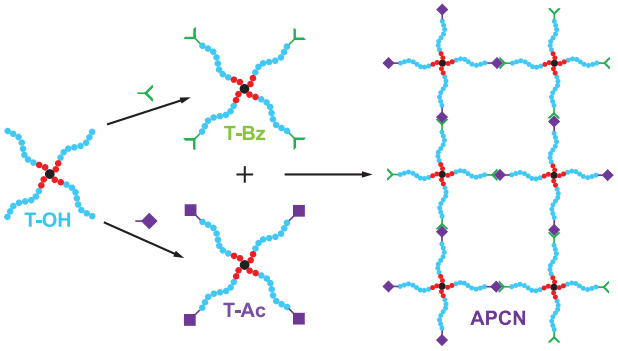


**FIGURE 2** | Schematic representation of the end-functionalization of the starting T1107 Tetronic four-armed star diblock copolymer to yield the two main polymeric building blocks, T-Bz and T-Ac, and their subsequent combination to mutually react and produce the APCN.

### 3.3 | APCN Ionogel Formulations and Films

Several APCN ionogel formulations were prepared, differing in terms of three important parameters. These samples were

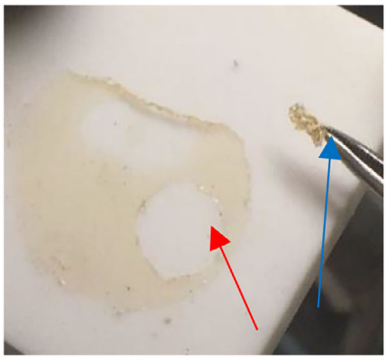

**FIGURE 3** | Sample cast on a PTFE plate from which a disk was cut (red arrow). After peeling the disk off the PTFE plate, the obtained membrane shrank and was stuck onto itself, leading to an unusable sample (blue arrow).

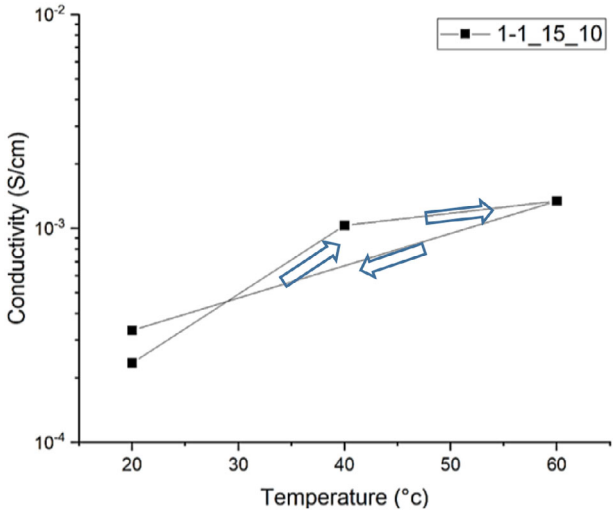


**FIGURE 4** | Conductivities of sample no. 10, 1-1_15_10, at different temperatures. The blue arrows show the direction of temperature change during the measurements. The error bars for the conductivity measurements were very small, of the size of the symbols in the figure.

subsequently evaluated for their electrochemical properties, and correlations were made between these properties and the values of the above-employed parameters. In particular, twelve formulations were prepared, in which the ratio (end-group stoichiometry) of the two polymer derivatives, the overall polymer concentration, and the acetic acid concentration were systematically varied. The main characteristics of these formulations have already been listed in Table 1 in the Experimental Section.

Table 1 shows that, within our experimental design, the T-Bz – T-Ac molar ratio was varied at five values, between 1:2 and 2:1, with 1:1 being the central value. On the other hand, the overall star polymer concentration was explored at four values, covering the range between 5 and 15% w/v, with 10% w/v being the central value, while the acetic acid catalyst concentration was studied at two values, most of them at 5% v/v. Each of the above solution mixtures (before their gelation) was cast on a stainless-steel disk (1.55 cm diameter, 0.5 mm thickness) and evaporated in a glove box for 24 h. Subsequently, each of the polymer membranes formed on top of the disk was transferred into a vacuum oven operated at 70°C where they were kept for 48 h for further drying and were finally transferred into the glove box to cool down to room temperature.

### 3.4 | Usable APCN Ionogel Films with a Drop Casting Method

For the conductivity measurements, the stainless steel disks with the polymer membranes were transferred into a CR2025 coin cell with two other stainless-steel disk spacers and one spring. The assembly was sealed under pressure. Sample no. 1, 1:1_5_5, is the one with the lowest polymer concentration, 5% w/v, and gave a film only after a very long time (>48 h) of drying, indicating a rather low crosslinking density in the membrane. Thus, we initially focused our study on samples with higher polymer concentrations, from 10% to 15% w/v. However, even the films obtained using these higher polymer concentrations, after their complete drying, they were not so strong and could be easily broken. Moreover, even if the drying procedure was done on a PTFE cup, it was impossible to remove the film with a good shape because it was too sticky to the PTFE and to itself, as shown in Figure 3. That is why we finally switched to a drop casting method on a stainless-steel disk, so as to analyze directly the conductivity of the film without the need for a self-standing film.

Only four samples gave satisfactory results, i.e., mechanically strong enough to be analyzed and allow for a normal impedance spectroscopy measurement, i.e., no short circuit. These samples are listed in Table 2 below.

### 3.5 | Ionic Conductivity

The conductivities obtained at room temperature were between 0.2 and 0.5 mS $cm^{-1}$, as compared to the conductivity of the IL in its pure form of around 6 mS $cm^{-1}$. In Figure 4, the conductivity

**TABLE 2** | Compositions of formulations that gave films with satisfactory mechanical strength allowing their electrochemical characterization.

| Sample | | T-Bz – T-Ac molar ratio | Total polymer concentration (% w/v) | Acetic acid concentration (% v/v) |
|---|---|---|---|---|
| No. | Name | | | |
| 1 | 1:1_5_5 | 1:1 | 5 | 5 |
| 5 | 2:3_10_5 | 1:1.5 | 10 | 5 |
| 10 | 1:1_15_10 | 1:1 | 15 | 10 |
| 11 | 1:2_11_5 | 1:2 | 11 | 5 |

**TABLE 3** | Room temperature conductivities measured for the four ionogel samples, as well as their ionic liquid volume fraction, and the reaction stoichiometry between the two star block building units.

| Sample | | Ionic conductivity (mS cm$^{-1}$) | T-Bz:T-Ac (mol/mol) | Ionic liquid content (% v/v) |
|---|---|---|---|---|
| No. | Name | | | |
| 1 | 1:1_5_5 | 0.27 | 1:1 | 58.1 |
| 5 | 2:3_10_5 | 0.43 | 2:3 | 41.2 |
| 10 | 1:1_15_10 | 0.24 | 1:1 | 32.1 |
| 11 | 1:2_11_5 | 0.13 | 1:2 | 38.7 |

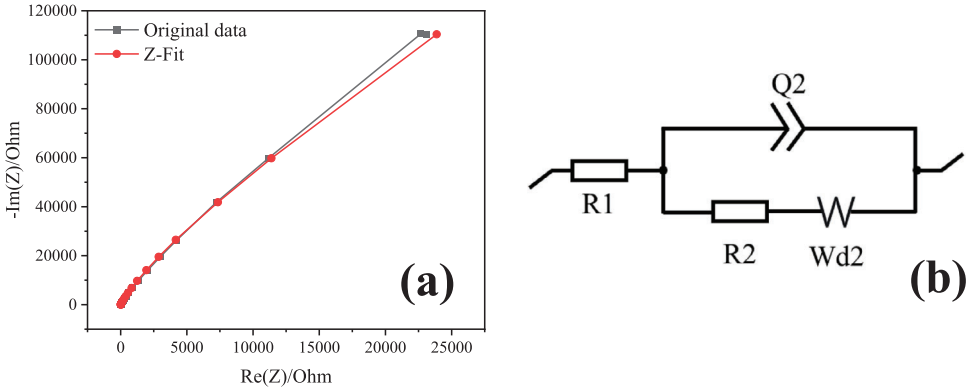


**FIGURE 5** | (a) Impedance spectrum for sample no. 5, 2:3_10_5, between 50 mHz and 0.1 MHz. The Z-fit (in red) shows the simulation to calculate the resistance which is 10.51 Ω. (b) Equivalent circuit used for the fitting. R1: solution resistance, representing the bulk (Ohmic) resistance of the electrolyte, characterizing the impedance to ion migration within the bulk material; R2: charge transfer resistance, quantifying the kinetic barrier to Faradaic reactions at the electrode-electrolyte interface; Q2: constant phase element, modeling the non-ideal capacitive behavior of the electrical double layer, typically resulting from surface roughness or heterogeneity; Wd2: Warburg impedance, characterizing the semi-infinite linear diffusion of ions in the electrolyte bulk, which becomes significant at lower frequencies due to concentration gradients established at the electrode surface.

of sample no. 10, 1:1_15_10, is shown at different temperatures, from 20°C to 60°C. Upon sample cooling from 60°C down to room temperature again, the measured conductivity was improved due to a better surface contact with the electrode.

The room temperature ionic conductivities of all four ionogel GPE samples without the heating cycle are listed in Table 3.

We observe that the highest conductivity is displayed by sample no. 5, 2:3_10_5. This may be attributed to a combination of two formulation properties, also listed in Table 3 above. The one property is the reaction stoichiometry between the two polymer derivatives, and the other is the content of the ionic liquid in the final ionogel (after DMF evaporation). Regarding the former property, it appears that deviation from perfect, 1:1, stoichiometry, may facilitate ion transport through a less compact ionogel. Regarding the latter property, it seems that a higher content of charge transporters (ions), through a higher volume fraction of ionic liquid, may also enhance the ion conductivity of the ionogel sample. It is noteworthy that sample no. 5 comes second in both of these two properties, off-stoichiometry ratio and highest ionic liquid volume fraction, but their combination, apparently, leads to optimal ion conductivity.

The above-mentioned room temperature highest ion conductivity of 0.43 mS cm$^{-1}$ for the present ionogel must be compared to that of the neat ionic liquid mixture of 6 mS cm$^{-1}$. The lower, by an order of magnitude, value of the ion conductivity of the best-performing ionogel compared to the free ionic liquid may be explained by considering the obstacles imposed to ion diffusion by the polymer matrix, which, nonetheless, converts the liquid electrolyte to a quasi-solid composite electrolyte. The room temperature ion conductivity of 0.43 mS cm$^{-1}$ for the present ionogel system is also lower than the corresponding value measured in our previous work (same ionic liquid mixture) on a (linear) Pluronic-based APCN ionogel of 2 mS cm$^{-1}$ [21], where the F108 Pluronic main building block possessed the same molar mass of 15 000 g mol$^{-1}$ and same PPG content of 20 mol% as the T1107 Tetronic in the present system. In this case, the higher ion conductivity value of the Pluronic-based ionogel may be attributed to the linear architecture of the Pluronic, possibly facilitating ion diffusion, which must be contrasted to the star-branched architecture of the presently used Tetronic, and also the higher ionic liquid volume fraction of 67% in the Pluronic system, as opposed to an ionic liquid volume fraction of 41% in the present system. Finally, the best room temperature ionic conductivity of the present ionogel system is comparable to the corresponding value from another previous study of ours (again same ionic liquid mixture used) on an ionogel based on end-linked tetraPEG and tetraPVDF of 0.6 mS cm$^{-1}$ at an ionic liquid volume fraction of 42.1% v/v [20].

We envision that our T1107-based GPE is microphase-separated, with the PPG minority (20 mol% PG units) component self-assembling into spheres which are devoid of IL, with the IL preferentially partitioning into the continuous and more polar PEG majority (80 mol% EG units) component. This distribution has been determined in a non-crosslinked Pluronic system, also swollen in an IL [62].

The impedance spectrum of sample no. 5 was subsequently recorded and is shown in Figure 5, together with the equivalent circuit used to analyze the data:

We saw that all Nyquist plots of the impedance data were linear, displaying no sign of high-frequency semicircles that would have been associated with a lack of homogeneity or a crystalline phase separation.

## 4 | Conclusions

A well-defined amphiphilic polymer conetwork (APCN) matrix was employed to house an ionic liquid mixture and obtain an APCN ionogel with potential application as a gel polymer electrolyte in lithium-ion batteries. The APCN matrix was based on end-linked T1107 Tetronic four-armed star diblock copolymer with shell blocks comprising poly(ethylene glycol) (PEG, 80 mol% EG units) and core blocks consisting of poly(propylene glycol) (PPG, 20 mol% PG units). The ionic liquid mixture was made of two organic salts, lithium bis(trifluoromethanesulfonyl)imide (LiTFSI) and 1-ethyl-3-methylimidazolium bis(trifluoromethanesulfonyl)imide (EMIM-TFSI), combined at a 1:9 molar ratio. Twelve different formulations of the APCN ionogel were prepared, and their films were, subsequently, characterized in terms of their ion conductivity. The measured room temperature ion conductivities ranged between 0.13 and 0.43 mS $cm^{-1}$, and were found to be comparable to those of similar APCN ionogels based on Pluronics or tetraPEG stars.


### Acknowledgements

The European Regional Development Fund and the Republic of Cyprus are acknowledged for co-funding this research work through The Research and Innovation Foundation of Cyprus (Project Acronym: DYNAmphiNET; Project Number: Excellence/0918/0325). Y. Z. and J.-F. G. are grateful to Service Public de Wallonie (Win4Excellence BATFACTORY 310153 project) for financial support.


### Conflicts of Interest

The authors declare no conflicts of interest.

### Data Availability Statement

The data that support the findings of this study are available from the corresponding author upon reasonable request.

### References


1. W. J. Hyun, C. M. Thomas, and M. C. Hersam, "Nanocomposite Ionogel Electrolytes for Solid-State Rechargeable Batteries," *Advanced Energy Materials* 10 (2020): 2002135, https://doi.org/10.1002/aenm.202002135.

2. Z. Luo, W. Li, J. Yan, and J. Sun, "Roles of Ionic Liquids in Adjusting Nature of Ionogels: A Mini Review," *Advanced Functional Materials* 32 (2022): 2203988, https://doi.org/10.1002/adfm.202203988.

3. X. Ma, J. Yu, Y. Hu, J. Texter, and F. Yan, "Ionic Liquid/Poly(Ionic Liquid)-Based Electrolytes for Lithium Batteries," *Industrial Chemistry & Materials* 1 (2023): 39–59, https://doi.org/10.1039/d2im00051b.

4. S. Zhang, J. Li, N. Jiang, et al., "Rational Design of an Ionic Liquid-Based Electrolyte With High Ionic Conductivity Towards Safe Lithium/Lithium-Ion Batteries," *Chemistry—An Asian Journal* 14 (2019): 2810–2814, https://doi.org/10.1002/asia.201900581.

5. I. Osada, H. de Vries, B. Scrosati, and S. Passerini, "Ionic-Liquid-Based Polymer Electrolytes for Battery Applications," *Angewandte Chemie International Edition* 55 (2016): 500–513, https://doi.org/10.1002/anie.201504971.

6. Y. Hu, L. Yu, T. Meng, S. Zhou, X. Sui, and X. Hu, "Hybrid Ionogel Electrolytes for Advanced Lithium Secondary Batteries: Developments and Challenges," *Chemistry—An Asian Journal* 17 (2022): 202200794, https://doi.org/10.1002/asia.202200794.

7. Y. Wei, W. Chen, X. Ge, et al., "A Flexible, Highly Conductive, Tough Ionogel Electrolyte Containing LiTFSI Salt and Ionic Liquid [EMIM][TFSI] Based on PVDF-HFP for High-Performance Supercapacitors," *Polymer* 289 (2023): 126501, https://doi.org/10.1016/j.polymer.2023.126501.

8. N. Chen, H. Zhang, L. Li, R. Chen, and S. Guo, "Ionogel Electrolytes for High-Performance Lithium Batteries: A Review," *Advanced Energy Materials* 8 (2018): 1702675, https://doi.org/10.1002/aenm.201702675.

9. D. S. Ashby, J. Cardenas, A. S. Bhandarkar, A. W. Cook, and A. A. Talin, "Modifying Ionogel Solid-Electrolytes for Complex Electrochemical Systems," *ACS Applied Energy Materials* 5 (2022): 12467–12474, https://doi.org/10.1021/acsaem.2c02085.

10. Z. Chen, Y. Yang, Q. Su, et al., "A Flexible Semi-Interpenetrating Network-Enhanced Ionogel Polymer Electrolyte for Highly Stable and Safe Lithium Metal Batteries," *ACS Applied Materials & Interfaces* 13 (2021): 41946–41955, https://doi.org/10.1021/acsami.1c07745.

11. L. Liang, X. Chen, W. Yuan, H. Chen, H. Liao, and Y. Zhang, "Highly Conductive, Flexible, and Nonflammable Double-Network Poly(Ionic Liquid)-Based Ionogel Electrolyte for Flexible Lithium-Ion Batteries," *ACS Applied Materials & Interfaces* 13 (2021): 25410–25420, https://doi.org/10.1021/acsami.1c06077.

12. K. Zhao, H. Song, X. Duan, Z. Wang, J. Liu, and X. Ba, "Novel Chemical Cross-Linked Ionogel Based on Acrylate Terminated Hyperbranched Polymer With Superior Ionic Conductivity for High Performance Lithium-Ion Batteries," *Polymers* 11 (2019): 444, https://doi.org/10.3390/polym11030444.

13. C. K. Varnava and C. S. Patrickios, "Polymer Networks One Hundred Years After the Macromolecular Hypothesis: A Tutorial Review," *Polymer* 215 (2021): 123322, https://doi.org/10.1016/j.polymer.2020.123322.

14. G. Hild, "Model Networks Based on 'Endlinking' Processes: Synthesis, Structure and Properties," *Progress in Polymer Science* 23 (1998): 1019–1149, https://doi.org/10.1016/S0079-6700(97)00055-5.

15. S. Nakagawa and N. Yoshie, "Star Polymer Networks: A Toolbox for Cross-Linked Polymers With Controlled Structure," *Polymer Chemistry* 13 (2022): 2074–2107, https://doi.org/10.1039/d1py01547h.

16. K. Fujii, H. Asai, T. Ueki, et al., "High-Performance Ion Gel With Tetra-PEG Network," *Soft Matter* 8 (2012): 1756–1759, https://doi.org/10.1039/c2sm07119c.

17. K. Hashimoto, K. Fujii, K. Nishi, T. Sakai, and M. Shibayama, "Nearly Ideal Polymer Network Ion Gel Prepared in pH-Buffering Ionic Liquid," *Macromolecules* 49 (2016): 344–352, https://doi.org/10.1021/acs.macromol.5b02360.

18. M. Yoshitake, Y. Kamiyama, K. Nishi, et al., "Defect-Free Network Formation and Swelling Behavior in Ionic Liquid-Based Electrolytes of Tetra-Arm Polymers Synthesized Using a Michael Addition Reaction,"

*Physical Chemistry Chemical Physics* 19 (2017): 29984–29990, https://doi.org/10.1039/c7cp06126a.

19. A. Ishikawa, T. Sakai, and K. Fujii, "An Ionic Liquid Gel With Ultralow Concentrations of Tetra-Arm Polymers: Gelation Kinetics and Mechanical and Ion-Conducting Properties," *Polymer* 166 (2019): 38–43, https://doi.org/10.1016/j.polymer.2019.01.044.

20. D. E. Apostolides, C. S. Patrickios, T. Sakai, et al., "Near-Model Amphiphilic Polymer Conetworks Based on Four-Arm Stars of Poly(Vinylidene Fluoride) and Poly(Ethylene Glycol): Synthesis and Characterization," *Macromolecules* 51 (2018): 2476–2488, https://doi.org/10.1021/acs.macromol.7b02475.

21. D. E. Apostolides, G. Michael, C. S. Patrickios, et al., "Dynamic Covalent Amphiphilic Polymer Conetworks Based on End-Linked Pluronic F108: Preparation, Characterization, and Evaluation as Matrices for Gel Polymer Electrolytes," *ACS Applied Materials & Interfaces* 16 (2024): 23813–23825, https://doi.org/10.1021/acsami.3c19189.

22. C. S. Patrickios and T. K. Georgiou, "Covalent Amphiphilic Polymer Networks," *Current Opinion in Colloid & Interface Science* 8 (2003): 76–85, https://doi.org/10.1016/S1359-0294(03)00005-0.

23. G. Erdodi and J. P. Kennedy, "Amphiphilic Conetworks: Definition, Synthesis, Applications," *Progress in Polymer Science* 31 (2006): 1–18, https://doi.org/10.1016/j.progpolymsci.2005.11.001.

24. L. Mespouille, J. L. Hedrick, and P. Dubois, "Expanding the Role of Chemistry to Produce New Amphiphilic Polymer (Co)Networks," *Soft Matter* 5 (2009): 4878–4892, https://doi.org/10.1039/b910041p.

25. C. S. Patrickios, ed., *Amphiphilic Polymer Co-Networks: Synthesis, Properties, Modelling and Applications* (Royal Society of Chemistry, 2020).

26. C. S. Patrickios and K. Matyjaszewski, "Amphiphilic Polymer Co-Networks: 32 Years Old and Growing Stronger—A Perspective," *Polymer International* 70 (2021): 10–13, https://doi.org/10.1002/pi.6138.

27. S. Dech, T. Cramer, R. Ladisch, N. Bruns, and J. C. Tiller, "Solid–Solid Interface Adsorption of Proteins and Enzymes in Nanophase-Separated Amphiphilic Conetworks," *Biomacromolecules* 12 (2011): 1594–1601, https://doi.org/10.1021/bm1015877.

28. I. Schoenfeld, S. Dech, B. Ryabenky, et al., "Investigations on Diffusion Limitations of Biocatalyzed Reactions in Amphiphilic Polymer Conetworks in Organic Solvents," *Biotechnology and Bioengineering* 110 (2013): 2333–2342, https://doi.org/10.1002/bit.24906.

29. H. Kamata, Y. Akagi, Y. Kayasuga-Kariya, U.-I. Chung, and T. Sakai, "Nonswellable′ Hydrogel Without Mechanical Hysteresis," *Science* 343, no. 6173 (2014): 873–875, https://doi.org/10.1126/science.1247811.

30. C. N. Walker, K. C. Bryson, R. C. Hayward, and G. N. Tew, "Wide Bicontinuous Compositional Windows From Co-Networks Made With Telechelic Macromonomers," *ACS Nano* 8 (2014): 12376–12385, https://doi.org/10.1021/nn505026a.

31. I. Sittko, K. Kremser, M. Roth, S. Kuehne, S. Stuhr, and J. C. Tiller, "Amphiphilic Polymer Conetworks With Defined Nanostructure and Tailored Swelling Behavior for Exploring the Activation of an Entrapped Lipase in Organic Solvents," *Polymer* 64 (2015): 122–129, https://doi.org/10.1016/j.polymer.2015.03.038.

32. C. Nardi Tironi, R. Graf, I. Lieberwirth, M. Klapper, and K. Müllen, "Synthesis and Selective Loading of Polyhydroxyethyl Methacrylate-*l*-Polysulfone Amphiphilic Polymer Conetworks," *ACS Macro Letters* 4 (2015): 1302–1306, https://doi.org/10.1021/acsmacrolett.5b00714.

33. S. Kondo, T. Hiroi, Y.-S. Han, et al., "Reliable Hydrogel With Mechanical "Fuse Link" in an Aqueous Environment," *Advanced Materials* 27 (2015): 7407–7411, https://doi.org/10.1002/adma.201503130.

34. T. Hiroi, S. Kondo, T. Sakai, et al., "Fabrication and Structural Characterization of Module-Assembled Amphiphilic Conetwork Gels," *Macromolecules* 49 (2016): 4940–4947, https://doi.org/10.1021/acs.macromol.6b00842.

35. K. R. McLeod and G. N. Tew, "Microphase-Separated Thiol–Ene Conetworks From Telechelic Macromonomers With Asymmetric Molecular Weights," *Macromolecules* 50 (2017): 8042–8047, https://doi.org/10.1021/acs.macromol.7b01681.

36. D. Gu, S. Tan, C. Xu, A. J. O'Connor, and G. G. Qiao, "Engineering Tough, Highly Compressible, Biodegradable Hydrogels by Tuning the Network Architecture," *Chemical Communications* 53 (2017): 6756–6759, https://doi.org/10.1039/c7cc02811c.

37. G. Guzman, S. S. Es-haghi, T. Nugay, and M. Cakmak, "Zero-Order Antibiotic Release From Multilayer Contact Lenses: Nonuniform Drug and Diffusivity Distributions Produce Constant-Rate Drug Delivery," *Advanced Healthcare Materials* 6 (2017): 1600775, https://doi.org/10.1002/adhm.201600775.

38. A. K. S. Chandel, B. Nutan, I. H. Raval, and S. K. Jewrajka, "Self-Assembly of Partially Alkylated Dextran-Graft-poly[(2-dimethylamino)ethyl methacrylate] Copolymer Facilitating Hydrophobic/Hydrophilic Drug Delivery and Improving Conetwork Hydrogel Properties," *Biomacromolecules* 19 (2018): 1142–1153, https://doi.org/10.1021/acs.biomac.8b00015.

39. L. Benski, I. Viran, F. Katzenberg, and J. C. Tiller, "Small-Angle X-Ray Scattering Measurements on Amphiphilic Polymer Conetworks Swollen in Orthogonal Solvents," *Macromolecular Chemistry and Physics* 222 (2021): 2000292, https://doi.org/10.1002/macp.202000292.

40. S. A. Wilhelm, M. Maricanov, V. Brandt, F. Katzenberg, and J. C. Tiller, "Amphiphilic Polymer Conetworks With Ideal and Non-Ideal Swelling Behavior Demonstrated by Small Angle X-Ray Scattering," *Polymer* 242 (2022): 124582, https://doi.org/10.1016/j.polymer.2022.124582.

41. K. Lee, Y. Shang, V. A. Bobrin, et al., "3D Printing Nanostructured Solid Polymer Electrolytes With High Modulus and Conductivity," *Advanced Materials* 34 (2022): 2204816, https://doi.org/10.1002/adma.202204816.

42. S. T. R. Velasquez, D. Jang, P. Jenkins, et al., "Peptide-Reinforced Amphiphilic Polymer Conetworks," *Advanced Functional Materials* 32 (2022): 2207317, https://doi.org/10.1002/adfm.202207317.

43. L. Löser, C. Bunk, R. Scholz, M. Lang, F. Böhme, and K. Saalwächter, "Structural Characterization of Amphiphilic Conetworks in Selective and Nonselective Solvents Using $^{1}$H NMR and SAXS," *Macromolecules* 57 (2024): 940–954, https://doi.org/10.1021/acs.macromol.3c02139.

44. S. T. R. Velasquez, A. Belluati, E. Tervoort, et al., "Microfluidically Produced Microcapsules With Amphiphilic Polymer Conetwork Shells," *Advanced Materials Technologies* 9 (2024): 2400109, https://doi.org/10.1002/admt.202400109.

45. N. Fribiczer, K. Hagmann, C. Bunk, F. Böhme, R. von Klitzing, and S. Seiffert, "Impact of Swelling on Macroscopic and Nanoscopic Mechanical Properties of Amphiphilic Polymer Co-Networks in Non-Selective and Selective Solvents," *Macromolecular Chemistry and Physics* 225 (2024): 2300389, https://doi.org/10.1002/macp.202300389.

46. D. E. Apostolides, G. Michael, C. S. Patrickios, et al., "The First Example of a Model Amphiphilic Polymer Conetwork Containing a Hydrophobic Oligopeptide: The Case of End-Linked Tetra[Poly(ethylene glycol)-b-oligo(L-alanine)]," *Gels* 11 (2025): 331, https://doi.org/10.3390/gels11050331.

47. S. T. R. Velasquez, D. Jang, J. Thomas, P. Grysan, L. T. J. Korley, and N. Bruns, "Advanced Mechanical Properties of Amphiphilic Polymer Conetworks Through Hierarchical Reinforcement With Peptides and Cellulose Nanocrystals," *Polymer Chemistry* 16 (2025): 2618–2628, https://doi.org/10.1039/d4py01283f.

48. A. Petróczy, I. Szanka, L. Bereczki, N. Hegyesi, J. Madarász, and B. Iván, "The Scissors Effect of the Macromolecular Crosslinker on the Glass Transition of Polystyrene in its Conetworks With Poly(dimethylsiloxane)," *Polymers* 17 (2025): 1656, https://doi.org/10.3390/polym17121656.

49. A. Petróczy, I. Szanka, A. Wacha, et al., "Bicontinuous Nanophasic Conetworks of Polystyrene With Poly(dimethylsiloxane) and Divinylbenzene: From Macrocrosslinked to Hypercrosslinked Double-Hydrophobic Conetworks and Their Organogels With Solvent-Selective Swelling," *Gels* 11 (2025): 318, https://doi.org/10.3390/gels11050318.

50. D. E. Apostolides, G. Michael, K. Andronikou, et al., "Synthesis of Highly Ordered Amphiphilic Polymer Conetwork Hydrogels via the Topologically Precise Interconnection of Two Highly Incompatible Polymers," *Chemistry of Materials* 37 (2025): 5515–5528, https://doi.org/10.1021/acs.chemmater.5c00127.

51. Z. Liu, Y. Zhang, C. S. Patrickios, and J. Jin, "Synthesis of Amphiphilic Polymer Co-Networks via the Growth of a Living RAFT Network," *Macromolecular Chemistry and Physics* 226 (2025): 2500004, https://doi.org/10.1002/macp.202500004.

52. S. Seitel, N. P. Lopez, S. Ihmann, F. Böhme, and S. Seiffert, "Diffusive Probe Penetration for Characterization of Diffusion-Governing Length Scales in Amphiphilic PEG–PCL Co-Networks," *Soft Matter* 21 (2025): 7860–7871, https://doi.org/10.1039/d5sm00629e.

53. J. Puig-Rigall, M. J. Blanco-Prieto, A. Radulescu, C. A. Dreiss, and G. González-Gaitano, "Morphology, Gelation and Cytotoxicity Evaluation of D-α-Tocopheryl Polyethylene Glycol Succinate (TPGS)—Tetronic Mixed Micelles," *Journal of Colloid and Interface Science* 582 (2021): 353–363, https://doi.org/10.1016/j.jcis.2020.08.004.

54. K. Mortensen and M. Annaka, "Structural Study of Four-Armed Amphiphilic Star-Block Copolymers: Pristine and End-Linked Tetronic T1307," *ACS Macro Letters* 5 (2016): 224–228, https://doi.org/10.1021/acsmacrolett.5b00936.

55. M. Fujiki, M. Ito, K. Mortensen, S. Yashima, M. Tokita, and M. Annaka, "Friction Coefficient of Well-Defined Hydrogel Networks," *Macromolecules* 49 (2016): 634–642, https://doi.org/10.1021/acs.macromol.5b01997.

56. K. Mortensen and M. Annaka, "Stretching PEO–PPO Type of Star Block Copolymer Gels: Rheology and Small-Angle Scattering," *ACS Macro Letters* 7 (2018): 1438–1442, https://doi.org/10.1021/acsmacrolett.8b00792.

57. D. E. Apostolides, C. S. Patrickios, M. Simon, et al., "Model Dynamic Covalent Thermoresponsive Amphiphilic Polymer Co-Networks Based on Acylhydrazone End-Linked Tetronic T904 Star Block Copolymers," *Polymer Chemistry* 14 (2023): 201–211, https://doi.org/10.1039/d2py01256a.

58. D. E. Apostolides, T. Sakai, and C. S. Patrickios, "Dynamic Covalent Star Poly(ethylene glycol) Model Hydrogels: A New Platform for Mechanically Robust, Multifunctional Materials," *Macromolecules* 50 (2017): 2155–2164, https://doi.org/10.1021/acs.macromol.7b00236.

59. W. P. Jencks, "Studies on the Mechanism of Oxime and Semicarbazone Formation 1," *Journal of the American Chemical Society* 81 (1959): 475–481, https://doi.org/10.1021/ja01511a053.

60. J. M. Sayer and W. P. Jencks, "General Base Catalysis of Thiosemicarbazone Formation," *Journal of the American Chemical Society* 91 (1969): 6353–6361, https://doi.org/10.1021/ja01051a029.

61. D. E. Apostolides and C. S. Patrickios, "Dynamic Covalent Polymer Hydrogels and Organogels Crosslinked Through Acylhydrazone Bonds: Synthesis, Characterization and Applications," *Polymer International* 67 (2018): 627–649, https://doi.org/10.1002/pi.5554.

62. A. Tsoutsoura, Z. He, and P. Alexandridis, "Effects of Ionic Liquids on the Cylindrical Self-Assemblies Formed by Poly(ethylene oxide)–Poly(propylene oxide)–Poly(ethylene oxide) Block Copolymers in Water," *Polymers* 16 (2024): 349, https://doi.org/10.3390/polym16030349.